Novel hybrid materials in the remediation of ground waters contaminated with As(III) and As(V)

Diwakar Tiwari [a], Seung Mok Lee [b,*]

[a] Department of Chemistry, School of Physical Sciences, Mizoram University, Aizawl 796 004, India
[b] Department of Environmental Engineering, Kwandong University, 522, Naegok-dong, Gangneung, Gangwondo 210-701, Republic of Korea

HIGHLIGHTS

► Novel hybrid inorgano–organo-modified sericite was obtained.
► The materials were characterized by IR, SEM and XRD data.
► Materials were utilized in the treatment of wastewater.
► Batch and column reactor operations.
► Effective removal of As(III) and As(V) from aqueous solutions.

GRAPHICAL ABSTRACT
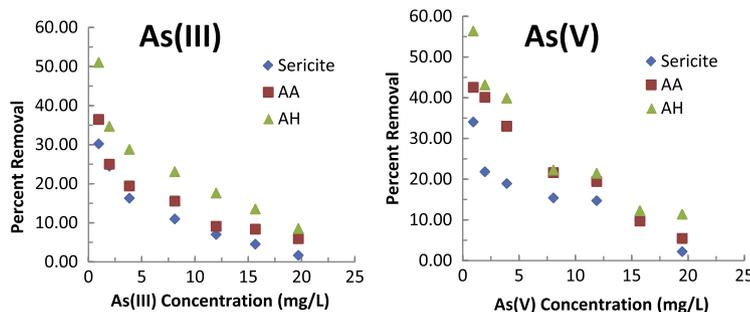
ABSTRACT

Natural mica type of clay mineral sericite was modified to obtain the materials *viz.*, Al-HDTMA-sericite (AH) and Al-AMBA-sericite (AA) which was characterized by the FT-IR and XRD data and morphologically analyzed by the SEM images. Further, the simulated batch reactor data indicated that increase in sorptive concentration enhanced the uptake of these pollutants and the 1000 times increase in ionic strength i.e., background electrolyte concentration ($NaNO_3$) caused an insignificant decrease in As(V) removal, which inferred that As(V) was adsorbed specifically onto the solid surface. However, it was affected greatly with As(III) pointed that As(III) was sorbed mainly through electrostatic or even with van der Waals attraction. pH dependence data showed that arsenic removal was greatly affected with change in solution pH. Simultaneous presence of phenol in the removal of As(III) or As(V) showed insignificant change in arsenic removal by these materials pointed that different sorption sites available for these two different contaminants. Results obtained under dynamic conditions inferred that materials were reasonably useful in the speciation/attenuation of these two metal ions from water bodies. The breakthrough data was fitted well to the Thomas equation and hence, the maximum amount of the As(III) or As(V) to be loaded was found to be 0.338 and 0.433 mg/g respectively for AA and AH for As(III) and 0.541 and 0.852 mg/g respectively for AA and AH for As(V) under the specified column reactor conditions. Comparing these two materials AH possessed with higher removal capacity than AA, at least, for these two contaminants.

© 2012 Elsevier B.V. All rights reserved.

1. Introduction

Arsenic contamination of ground waters is now termed as global environmental issue and the countries like Bangladesh, India, USA, China, Mexico, Taiwan, etc. are affected greatly [1–3]. Several geological/weathering reactions, volcanic emissions resulted in the arsenic mobilization in the natural environment. It was reported that soil erosion and leaching could contribute to 612×10^8 and 2380×10^8 g/year or total arsenic, respectively in the dissolved and suspended forms received by the oceans [4]. The additional sources of arsenic mobilization in the environment were mining activities, combustion of fossil fuels, use of arsenic pesticides, herbicides and crop desiccants, etc.

* Corresponding author. Tel.: +82 33 649 7535; fax: +82 33 642 7635.
E-mail addresses: diw_tiwari@yahoo.com (D. Tiwari), leesm@kwandong.ac.kr (S.M. Lee).

Arsenic exposure caused for the vomiting, esophageal and abdominal pain and bloody 'rice water' diarrhea [5–8]. However, the acute arsenic poisoning was reported as skin, lung, bladder and kidney cancer as well as pigmentation changes, skin thickening (hyperkeratosis) neurological disorder, muscular weakness, loss of appetite and nausea [5,9,10].

Clay and minerals are known natural materials and perhaps used for arsenic decontamination however, the sorption capacity of these materials was found to be insignificant. Additionally, these materials possessed with low settling properties hence, limiting its practical implication in such purposes. Therefore, the search for newer materials prompted us to modify/functionalize the clay materials in specific sorption of arsenic. Variety of organo-clay materials were introduced, and showed fairly good organophilic behavior and found to be effective in organic pollutants attenuation however, the inorganic pollutants in particular the anionic oxyanions were not to be treated effectively with these oragno-modify clay materials [11]. Li and Bowman [12], although, used the natural kaolinite modified with HDTMA for the retention of several inorganic oxyanions *viz.*, nitrate, arsenate and chromate. The mechanism of these oxyanion's sorption onto this organo-kao-linite was suggested as given below:

$$x(HDTMA - Clay - Br) + AO_y^{x-} = (HDTMA - Clay)_x - AO_y + xBr^-$$
(1)
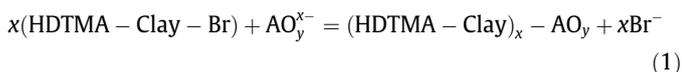
where 'A' referred either N, Cr or As.

Further, the newer hybrid materials obtained by inorgano–organo-clay showed enhance applicability as it could not only to be effective for the inorganic ion removal but also showed fair affinity to remove organic impurity simultaneously from aqueous wastes. In a line silylated pillared bentonite (SPILC) was obtained as inorgano–organo-composite [13]. The two step preparation process caused an increase in basal spacing from 1.53 nm (bentonite) to 1.95 nm (OTS-Al-PILC). Moreover, the pillaring of the clay materials with the inorganic metals *viz.*, Al, Fe, Cr, Ti, etc. enhanced significantly the settling property of clay however, showed very little affinity towards the organics in the aqueous solutions. However, the partial/or complete modification of theses intercalated clays with organic cationic surfactants possessed fairly a good sorption capacity even for the organic pollutants as well [14–16]. Important features of these inorgano–organo-clays were reported that they possessed two different sorption sites capable of removing different types of pollutants i.e., organic and inorganic pollutants from the aqueous solutions simultaneously, with an enhanced sorption capacity [17,18].

The interlayer pillared clay obtained with the pillaring inorganic polycations *viz.*, Al (Al—B) and Cr (Cr—B) with bentonite (B = bentonite) were used to remove the Supranol Yellow 4GL from aqueous solutions [19]. Further, the surfactant treated Al and Cr was intercalated within the bentonite interlayer showed an enhanced sorption capacity for this dye. The sorption data fitted well to the Langmuir adsorption isotherm. Similar, pillaring of montmorillonite was carried out with Al(III), Fe(III) and Ti(IV), and followed by co-adsorption of cetyl trimethylammonium bromide (CTA) [20]. These materials were then used for the removal of diuron (3-(3,4-dichlorophenyl)-1,1-dimethylurea and its degradation products (*viz.*, 3-(3,4-dichlorophenyl)-1-methylurea; 1-(3,4-dicholorophenyl)urea; 2,4-dichloroaniline). The removal efficiency of these solids was in the order of CTA-Ti$_x$H$_y$-montm > CTA-Fe$_x$(OH)$_y$-montm > CTA-Al$_x$(OH)$_y$-montm towards these pesticides. The mechanism of these pesticides sorption onto the organo–inorgano-clays was suggested as van der Waals attraction between the pesticides and the alkyl chains of the CTA cations, in part, on the surface of solids and to a greater extent on the interlamellar polycations. Earlier, we already have used sericite, mica based clay

mineral abundantly available in Korea, in the removal/speciation of two important inorganic cations *viz.*, Cu(II) and Pb(II) from aqueous solutions [21]. Further, the sericite was modified with HDTMA and AMBA as to obtain organo-sericite and was employed in the removal of phenol from aqueous solutions under batch reactor operations [22]. These studies inferred that the suitable modification of sericite could enable it for further environmental applications. Hence, keeping in view the wider use of inorgano–organo-clay materials, the present communication dealt to obtain novel inorgano–organo-sericite materials which were then employed for the removal of As(III) and As(V) from aqueous solutions.

2. Materials and methods

2.1. Materials

Sericite was obtained from the Keumnam deposit, Gagokmyun, Samcheok City, Kangwon province, Korea. It was crushed and sieved to obtain 200–300 BSS (British Standard sieve i.e., 0.075–0.053 mm) mesh size by using a mechanical sieve. This was washed with purified water, dried and crushed in mortar for its further use. The cation exchange capacity (CEC) of sericite was obtained by the US EPA method 9080 (http://www.epa.gov/osw/hazard/testmethods/sw846/pdfs/9080.pdf) and was found to be 8.85 meq/100 g of sericite. Sericite was contained with various metal oxides [21]. Hexadecyltrimethylammonium bromide (HDTMA) was obtained from Sigma–Aldrich, USA. Alkyldimethylbenzylammonium chloride (AMBA) 50% solution, and aluminum(III) chloride both were obtained from Junsei Chemical Co. Ltd., Japan. Sodium meta arsenite and disodium hydrogen arsenate heptahydrate were obtained from Wako Pure Chemical Industries Ltd. Japan. Sodium hydroxide and other chemicals used were of AR grade and the deionized water was further purified (18 MΩ cm) by using Millipore water purification system (Milli-Q+).

2.2. Methodology

2.2.1. Preparation of inorgano–organo-sericite
The aluminum pillared HDTMA or AMBA-modified sericite was obtained by the simple wet method. The pillaring solution was prepared by mixing 100 mL of 0.4 mol/L NaOH solutions to 100 mL of 0.2 mol/L AlCl₃ solutions under vigorous stirring. The solution mixture was kept for 7 days at room temperature. In this solution mixture a known amount of HDTMA/or AMBA solution (the HDTMA/or AMBA was taken as equivalent to 1:1 CEC of sericite) with continuous stirring. 4 g of sericite powder was taken separately into 300 mL of water and mixed with the HDTMA/or AMBA mixed aluminum solution under vigorous stirring. The solution was stirred for another 5 h at room temperature, and then it was kept at room temperature for another 2 days. The dispersion was separated manually and washed the solids with plenty of purified water. The obtained solids i.e., aluminum-HDTMA-sericite (AH) and Al-AMBA-sericite (AA) were dried at 50 °C and grounded gently in mortar.

2.2.2. Surface morphology and characterization of materials
The morphology of these inorgano–organo-sericite materials along with sericite was obtained by taking SEM (scanning electron microscope) images using the Model FE-SEM SU-70 (Hitachi, Japan). X-ray diffraction (XRD) data was obtained by using X-ray diffraction machine i.e., PANalytical, Netherland (Model X'Pert PRO MPD), which was collected with the scan rate of 0.034 of 2θ illumination at the applied voltage 45 kV and the current was observed 35 mA. The Cu Kα radiations was employed having wavelength

of 1.5418 Å. FT-IR (Bruker, Tensor 27, USA by KBR disk method) was used taking the IR data for these solids.

2.2.3. pH_{PZC} and BET measurements

The pH_{PZC} (point of zero charge) was determined by the method reported previously [23]. Similarly, the specific surface area of these solids was obtained by using the BET Analyzer Macsorb HM machine (Model-1201), Japan.

2.2.4. Batch reactor experiments

Stock solutions of As(III)/or As(V) 100 mg/L was prepared by dissolving an appropriate amount of respective arsenic salts in the purified water and the desired concentration was obtained by successive dilution of stock solution, however, the diluted solution concentration was again measured by the AAS (Fast Sequential Atomic Absorption Spectrometer: Model AA240FS, Varian). 2.0 mg/L of As(III)/or As(V) solution (40 mL) was taken into polyethylene bottles. The pH of these solutions was adjusted by drop-wise additions of conc. HNO$_3$/NaOH solutions. 0.2 g of solid i.e., inorgano–organo-modified sericite was then added into each bottles. The bottles were kept in an automatic shaker (KUKJE, Shaking Incubator, Korea model 36-SIN-125) for 24 h at constant temperature 25 ± 1 °C in order to complete the sorption process. An apparent equilibrium between solid/solution could therefore be achieved. The samples were taken out from the shaker and filtered by using 0.45 μm syringe filter and the pH was again checked and it was mentioned in throughout in the text. The filtrates were then subjected to its bulk sorptive concentration measurements using AAS. The percentage removal of arsenic was calculated using the following equation:

$$\% \text{ Removal} = \frac{C_0 - C_e}{C_0} \times 100 \tag{2}$$

where C_0 and C_e were the initial and bulk arsenic concentration, respectively.

The concentration dependence data was collected by taking sorptive concentration from 1 to 20 mg/L at a constant pH ~ 4.5 and at constant temperature 25 ± 1 °C. The sorption experiments were conducted as detailed before. The results were reported in terms of sorptive concentration and respective amount of arsenic removed. This equilibrium concentration dependence sorption data were further employed for the equilibrium modeling studies using the Freundlich and Langmuir adsorption isotherms equations as discussed elsewhere to its linear and non-linear forms [24,25].

Similarly, the ionic strength dependence study was conducted varying the background electrolyte concentration from 0.0001 to 0.1 mol/L of NaNO$_3$ solution. The sorptive pH (4.5) and temperature (25 ± 1 °C) was kept constant. The results were presented as percent removal with a function of ionic strength.

Presence of phenol in the arsenic (i.e., As(III)/or As(V)) was studied varying the phenol concentration from 0.5 to 2.0 mol/L while the sorptive concentration was kept constant i.e., 2.0 mg/L keeping constant temperature 25 ± 1 °C. The percent removal of As(III)/or As(V) against a phenol concentration was presented thereafter.

2.2.5. Column experiments

The column experiments were performed using a glass column (1 cm inner diameter) packed with 1 g of inorgano–organo-sericite (kept middle in the column); below and above to this, it was taken 2 g of virgin sericite particles (14-16 BSS) and then it was filled with glass beads. Sorptive solution of As(III)/or As(V) 2 mg/L having a constant pH 4.5 was pumped upward from the bottom of the column using Acuflow Series II, High-Pressure liquid chromatograph, at a constant flow rate of 1.00 mL/min. Effluent samples were then collected using Spectra/Chrom CF-1 fraction collector. The liquid

samples collected were filtered using a 0.45 μm syringe filter and the total bulk sorptive concentration was measured using AAS.

The breakthrough data was further utilized to optimize the removal capacity of these solids under the dynamic conditions using the Thomas Eq. (3) [26]:

$$\frac{C_e}{C_0} = \frac{1}{1 + e^{\frac{K_T(q_0 m - C_0 V)}{Q}}} \tag{3}$$

where C_e was As(III)/or As(V) concentration in the effluent (mg/L); C_0 was As(III)/or As(V) concentration in the feed (mg/L); K_T the Thomas rate constant (L/min/mg); q_0 was the maximum amount of As(III)/or As(V) could be loaded (mg/g) under the specified column conditions; m the mass of adsorbent loaded (g); V the throughput volume (L); and Q the flow rate of pumped sorptive solution (L/min). A non-linear regression was conducted using the column data by the least square fitting for two unknown parameters i.e., K_T and q_0.

3. Results and discussion

3.1. Surface morphology of solids

SEM images of sericite and inorgano–organo-modified sericite were shown in Fig. 1a–c respectively for the sericite, AA and AH solids. Sericite showed very compact, ordered and layered structure. It hardly found any micro- or meso-pores on its surface. On the other hand, however, the inorgano–organo-modified sericite showed very heterogeneous and disordered surface structure. The surface was propped-up to some extent, in presence of inorganic and organic ions. Some micro-pores were also visible. It was assumed that the water molecules or even the potassium ions present within the interspace of sericite were likely to be replaced by the aluminum ions as aluminum hydroxide and further incorporated the HDTMA or AMBA organo cations.

3.2. Characterization of solid samples

FT-IR spectra of the sericite along with inorgano–organo-modified clay were illustrated in Fig. 2. The IR stretching bands occurred at 3625 and 3472 cm^{-1} were attributed respectively to the hydroxyl groups present with clay sheets and the water molecules present within the interlayer space of sericite [27–29]. On the other hand AH and AA samples showed that the band occurred at 3472 cm^{-1} was decreased significantly or disappeared, which suggested that replacement of aluminum or even with organic molecule or these were grafted with the hydroxyl groups [30]. Moreover, the band occurred at 3625 cm^{-1} shifted more at higher frequency. Similarly, the appearance of very weak but new bands in the spectra of the modified clay, centered at 2929 cm^{-1} and 2856 cm^{-1} were considered as C—H stretching vibrations, and C—H scissoring bands respectively of HDTMA-sericite and AMBA-sericite [27]. Further a band at 1652 cm^{-1} with sericite inferred to characteristic of Al and Mg bound water molecule which was almost disappeared with modified sericite. A frequency band at 1041 cm^{-1} was assigned as asymmetric stretching vibrations of Si—O—Si of sericite. Also bands from 737 to 842 cm^{-1} were further referred as characteristic bands of quartz and bands in between 478 and 536 were assigned to OSiO bending vibrations incurred for sericite [31].

Further, the XRD data obtained for sericite and inorgano–organo-modified sericite i.e., AA and AH were shown in Fig. 3. Sericite showed distinct reflections at the 2θ values of 8.81, 17.88, 19.98, 20.97, 23.00, 23.91, 25.60, 26.74 and 27.99 which were very characteristic reflections of the sericite clay mineral [32]. Further, AA and AH showed almost similar reflections with slight changes.
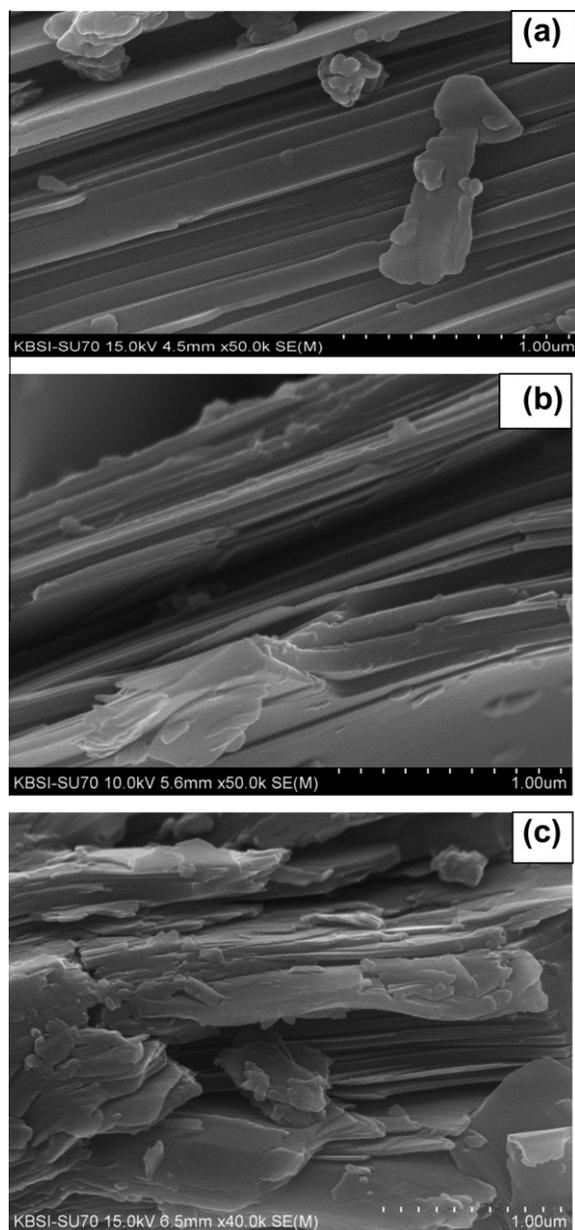
Fig. 1. SEM images of (a) sericite; (b) AH and (c) AA.

The *d*-values along with the relative intensities were obtained for these reflections. Sample AA showed a positive *d*-value difference which indicated that the interlayer of the sericite was propped up with some extent. These results were in a line to our previous findings where sand sample was modified with manganese dioxide [22]. On the other hand there was no significant change observed with the solid AH indicated that the interspace of sericite was not propped up.

3.3. pH_{PZC} and BET analysis

The pH_{PZC} was found to be 6.89, 6.30 and 6.20 respectively for the sericite, AH and AA samples. There is a significant decrease in the pH_{PZC} values noted with the modified sericite. On the other hand, the BET specific surface obtained was found to be 2.06, 1.712 and 0.928 m^2/g. It is evident with the BET data that the modified clay possessed with less specific surface area since the inorgano–organo molecules occupy the available pores of sericite or anchored within the interspace region.

3.4. Batch reactor experiments

3.4.1. Effect of pH

pH dependence data was obtained varying the sorptive initial pH from 2.00 to 10.00 for As(III)/or As(V) and the results were presented graphically in Fig. 4a and b respectively for As(III) and As(V). The percent uptakes of these two ions were presented with the final pH values in these figures. In general, it was noted that the percent removal of As(III) or As(V) was significantly low at high pH values. However, very high uptake was occurred for As(V) at moderate pH values i.e., pH 5.5. Moreover, low pH also favored the uptake of these two oxyanions. Quantitatively, increasing the pH from 1.98 to 9.16 caused for an apparent decrease in percent removal of As(III) respectively from 29.49% to 1.71% for AA. On the other hand increasing the pH from 1.95 to 8.72 caused to decrease in percent removal of As(III) respectively from 43.59% to 4.27% for AH. Similarly, the percent removal of As(V) was decreased from 22.67 to 14.22 for (AA) and 24.89 to 20.00 for (AH) for the respective increase in pH from 2.05 to 9.18 (for AA) and 1.93 to 9.18 (for AH). These results could better explain with the help of speciation of As(III) and As(V) in aqueous solutions as well the surface behavior of these solids.

Fig. 4a clearly demonstrated that the uptake of As(III) was relatively high at low pH values i.e., at pH 2.0 which was decreased gradually increasing the solution pH and almost negligible amount of arsenic was removed at very high pH i.e., at 9.8. However, a sharp decrease in the uptake of As(III) was occurred at pH around 6.0. This could be explicable with the fact that both these solids i.e., AA and AH becomes negatively charged above the pH_{PZC} values respectively 6.20 and 6.30, which rendered for this sharp decrease of As(III) uptake. The high uptake of arsenic at very low pH values was demonstrated because the surface of the solids likely to be positively charged at low pH (~2.0) values which could facilitate to attract electrostatically the negatively charged meta-arsenite in solution AsO_2^-. Further, gradual decrease in As(III) uptake within the pH region (~2.0–6.0) indicated that HDTMA and AMBA was less involved in the removal process which was again confirmed with the effect of phenol concentration studies described in proceeding sections. Similar, electrostatic attraction was reported previously for the sorption of As(III) by hybrid materials as well the other studies conducted by the soil samples as well [33–35]. Moreover, the uptake of H_3AsO_3 species by the iron modified sand was reported to be attracted by the van der Waals attraction [36].

On the other hand, the uptake of As(V) was greatly affected with pH and it was observed that increasing the pH from 2 to 6 the uptake of As(V) was increased both for AA and AH solids, however, beyond pH 6 it was decreased significantly. This may be explicable with the fact that at low pH values the surface carries positive charge and part of the As(V) was uncharged species hence, the interaction was restricted to some extent. However, with the increase of pH, the speciation studies [37] showed that in the intermediate region of pH i.e., pH 5.0–6.5 both these anionic species i.e., $H_2AsO_4^-$ and $HAsO_4^{2-}$ contribute to total arsenic concentration, which greatly facilitate in the attraction followed by perhaps the 'ion- exchange' or even the inner sphere complexation of the arsenic species with the aluminum oxide. The probable mechanism was proposed as specific arsenic sorption and OH$^-$ release from the surface [38]. It was also reported that inorgano–organo-clay showed anion/OH$^-$ exchange reaction for phosphate sorption [17] and mentioned that the phosphate removal was decreased gradually with the increase in solution pH which was attributed because not only due to increase in OH$^-$ concentration but also due to change in surface charge to negative as well in increase of the binding strength of —OH on metal.

However, beyond pH 6.5 the surface becomes negatively charged, since the pH_{PZC} values obtained 6.20 and 6.30 respectively
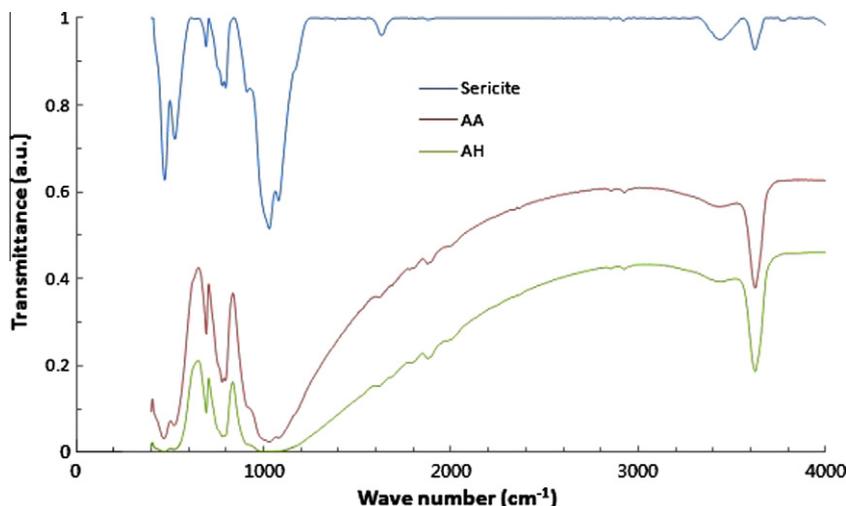
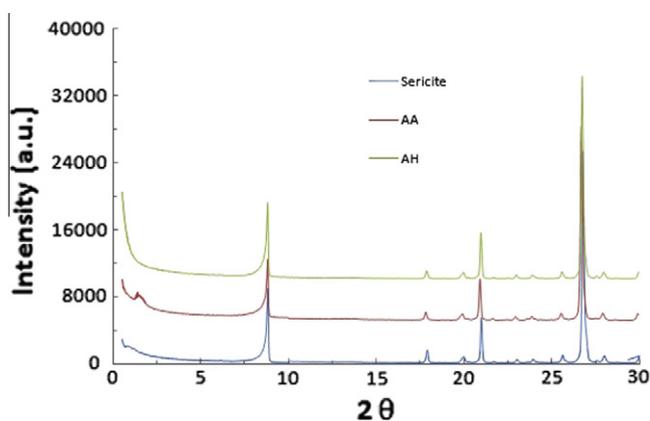**Fig. 2.** FT-IR spectra for the sericite and AH and AA.

Fig. 3. XRD pattern of sericite, AH and AA.

for AA and AH, and the arsenic species were also negatively charged hence greatly hampered the further uptake of the arsenic oxyanion.

3.4.2. Effect of sorptive concentration

As(III)/or As(V) concentration was increased from 1 mg/L to 20 mg/L at constant pH 4.5. The results were presented graphically as amount of As(III) or As(V) removed as a function of sorptive concentration (cf Fig. 5a and b respectively for As(III) and As(V)). The data was also included with the virgin sericite as to compare the efficiency of the modified solid. It was noted AH and AA possessed higher removal percentage than sericite throughout the studied sorptive concentrations. It further showed that increasing the sorp-

tive concentration from 1 to 20 mg/L caused to an substantive decrease in percent uptake of As(III) or As(V) by these solids. This could be explicable with the fact that at low arsenic concentrations more and more active sites were available for relatively smaller number of sorbing species. However, at higher sorptive concentration comparably lesser number of active sites were available for very large number of sorbing ions [21,24].

3.4.3. Equilibrium modeling

The concentration dependence study was further utilized to model it towards the known Freundlich and Langmuir adsorption isotherm to its linear and non-linear equations. The Freundlich model which was assumed to the basic assumptions that sorption occurred on an energetically heterogeneous solid surface on which the sorbed species were interacted laterally. On the other hand, the Langmuir model assumed that active sites were energetically homogeneously distributed onto the solid surface and the adsorbing species aggregated forming monolayer coverage onto the surface. The equilibrium concentration dependence data were fitted to the standard Freundlich and Langmuir adsorption linear equation and the Freundlich and Langmuir constants were estimated. These constants along with the R^2 values were returned in Table 1. The fitting data clearly indicated the applicability of these two models studied. Additionally, a non-linear fitting of the equilibrium state sorption data was fitted and solved using the solver add-in with Microsoft's spreadsheet using Microsoft Excel. The results obtained were returned in Table 2. Further, the results obtained by the two different way of data fitting showed insignificant difference. Moreover, the marked difference in capacity estimated by these two models i.e., Freundlich and Langmuir was attributed to the different basic nature and assumptions of the models. However, it was inferred that the modified sericite

Table 1
Freundlich and Langmuir adsorption isotherms constants estimated for the sorption of As(III) and As(V) by sericite, AH and AA solids using linear adsorption equations.

System	Freundlich isotherm			Langmuir isotherm		
	$K_f \pm 3.\sigma$	$1/n \pm 3.\sigma$	R^2	$q_m \pm 3.\sigma$	$b \pm 3.\sigma$	R^2
Sericite-As(III)	0.0777 ± 0.0002	0.416 ± 0.003	0.858	0.1616 ± 0.0003	1.440 ± 0.008	0.968
AA-As(III)	0.0899 ± 0.0003	0.392 ± 0.002	0.922	0.2720 ± 0.0004	0.5082 ± 0.004	0.977
AH-As(III)	0.1385 ± 0.0004	0.314 ± 0.003	0.829	0.4095 ± 0.0003	0.6857 ± 0.005	0.944
Sericite-As(V)	0.0775 ± 0.0002	0.580 ± 0.005	0.969	0.4643 ± 0.0004	0.1801 ± 0.003	0.921
AA-As(V)	0.1320 ± 0.0004	0.503 ± 0.004	0.928	0.4844 ± 0.0005	0.4311 ± 0.004	0.964
AH-As(V)	0.1699 ± 0.0005	0.438 ± 0.003	0.941	0.5340 ± 0.0004	0.5101 ± 0.005	0.969

(a)

(b)

Fig. 4. Effect of pH in the removal of (a) As(III); and (b) As(V) using inorgano–organo-modified sericite.

(a)

(b)

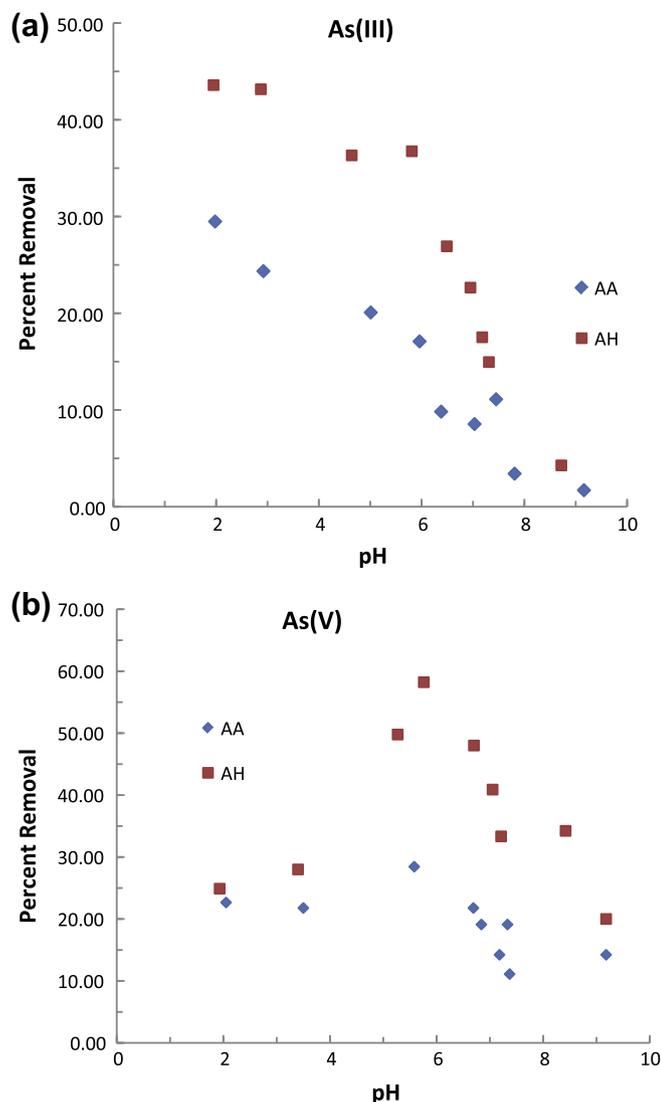**Fig. 5.** Effect of sorptive concentration in the removal of (a) As(III); and (b) As(V) using sericite and inorgano–organo-modified sericite.

possessed with significantly higher removal capacity compared to the virgin sericite sample. Comparing to AH and AA, AH showed higher sorption capacity and it was found to be more than two times higher than the capacity of sericite sample. Moreover, the Freundlich constants $1/n$, which was termed to the adsorption intensity, possessed with fractional values for these systems pointed it towards the heterogeneous nature of the solid surface along with exponential distribution of sorption/active sites [24,39,40].

Similarly, the Langmuir constant '*b*' reflected to the strength and affinity of the solids towards the sorbing species [41]. It also was related to an equilibrium constant of the process uptake process as: As(III)/or As(V) + Solid Surface → As(III)/or As(V)....Solid (surface adsorption complex).

3.4.4. Effect of background electrolyte concentration

In order to demonstrate the specific and non-specific adsorption, the effect of background electrolyte concentration could perhaps assist to explain it [42]. It was reported that the specific sorption was unaffected with the change in ionic strength, whereas the non-specific adsorption was influenced greatly by the change of ionic strength because of the competitive adsorption with coun-
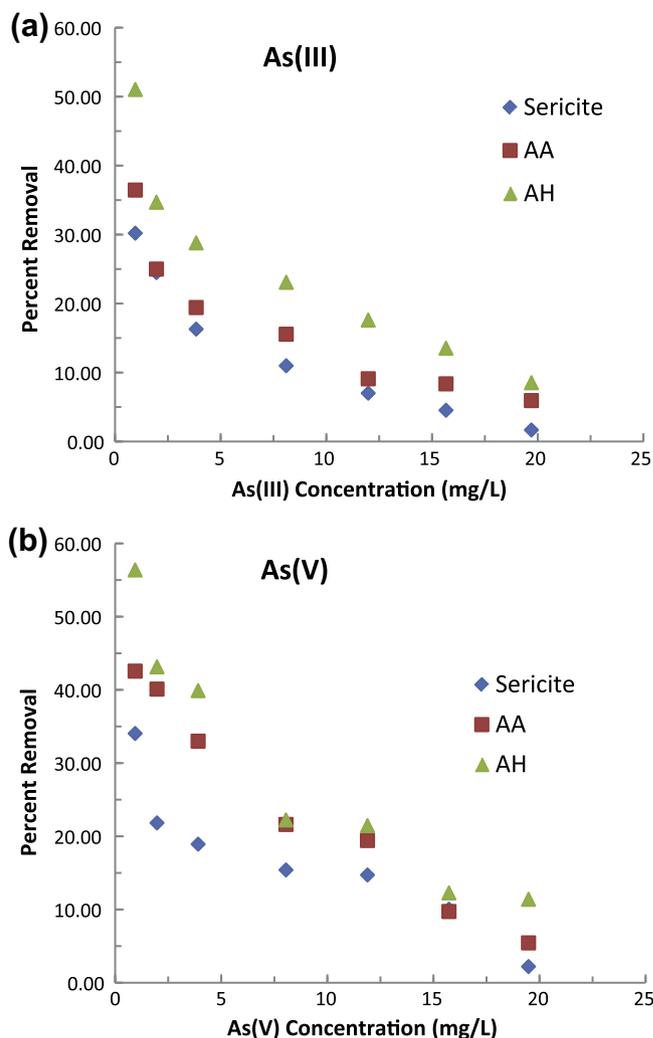
ter ions. Hence keeping in view the study was extended to observe the change of background electrolyte concentration i.e., NaNO$_3$ in the sorption behavior of these solids at least for the removal of studied oxyanions at constant pH 4.5. The Background concentration was increased from 0.0001 to 0.1 mol/L of NaNO$_3$ (1000 times) and the corresponding percent removal of As(III)/or As(V) was presented graphically in Fig. 6a and b respectively for As(III) and As(V). Quantitatively, it was observed that increasing the background concentration from 0.0001 to 0.1 mol/L NaNO$_3$ (i.e., 1000 times increase) caused for decrease of the As(III) uptake respectively from 66.48% to 23.08% for AA i.e., 43.4% decrease and 56.59% to 26.37% i.e., 30.22%. Similarly the uptake of As(V) was decreased from 58.72% to 46.54% for AA i.e., 12.18% decrease; 57.34% to 48.85% for AH i.e., 8.49% decrease, respectively for the increase of background electrolyte concentration from 0.0001 to 0.1 mol/L NaNO$_3$. These results demonstrated that the 1000 times increase of background electrolyte concentration caused insignificantly the decrease of As(V) sorption onto these solid materials pointed that sorbing ions were sorbed specifically and forming an inner sphere complexation with the surface active sites. Hence, it favored that these oxyanions were mostly sorbed with the aluminum oxides which was introduced within the interspace of sericite. On the other hand the sorption of As(III) sorption onto the AA and AH solids was greatly hampered with the background electrolyte concen-

Table 2
Freundlich and Langmuir adsorption isotherms constants estimated for the sorption of As(III) and As(V) by sericite, AH and AA solids using non-linear adsorption equations.
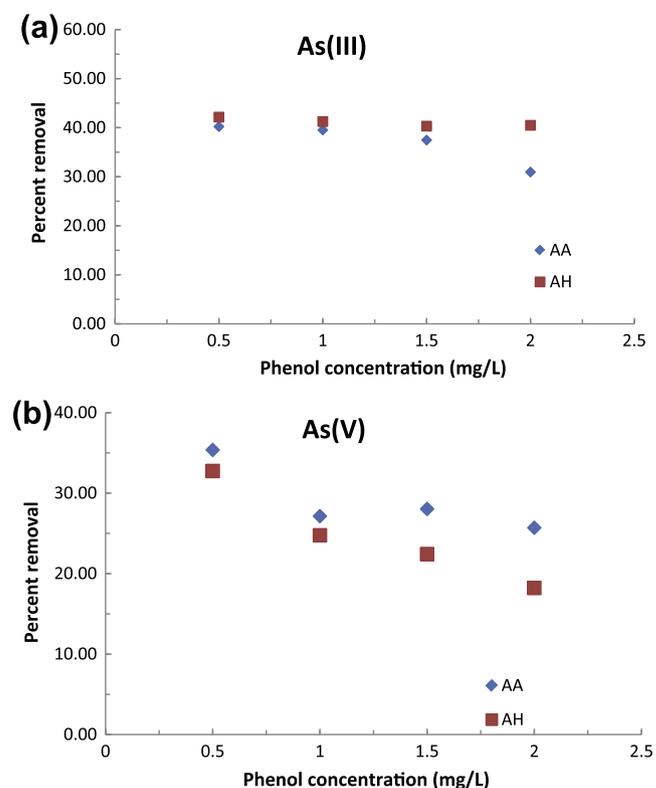
System	Freundlich isotherm			Langmuir isotherm		
	$K_f \pm 3.\sigma$	$1/n \pm 3.\sigma$	Least square sum $\times 10^{-3}$	$q_m \pm 3.\sigma$	$b \pm 3.\sigma$	Least square sum $\times 10^{-3}$
Sericite-As(III)	0.0873 ± 0.0002	0.252 ± 0.002	2.66	0.1412 ± 0.0006	0.785 ± 0.005	1.20
AA-As(III)	0.1031 ± 0.0004	0.328 ± 0.004	5.55	0.1224 ± 0.005	0.428 ± 0.004	2.97
AH-As(III)	0.1655 ± 0.0005	0.333 ± 0.003	22.75	0.1958 ± 0.0006	0.420 ± 0.004	12.0
Sericite-As(V)	0.0689 ± 0.0004	0.596 ± 0.005	4.41	0.0580 ± 0.0002	0.105 ± 0.003	3.12
AA-As(V)	0.1596 ± 0.0005	0.398 ± 0.004	12.42	0.1988 ± 0.0004	0.391 ± 0.005	5.80
AH-As(V)	0.1903 ± 0.0006	0.374 ± 0.005	12.54	0.2627 ± 0.0004	0.481 ± 0.004	8.44
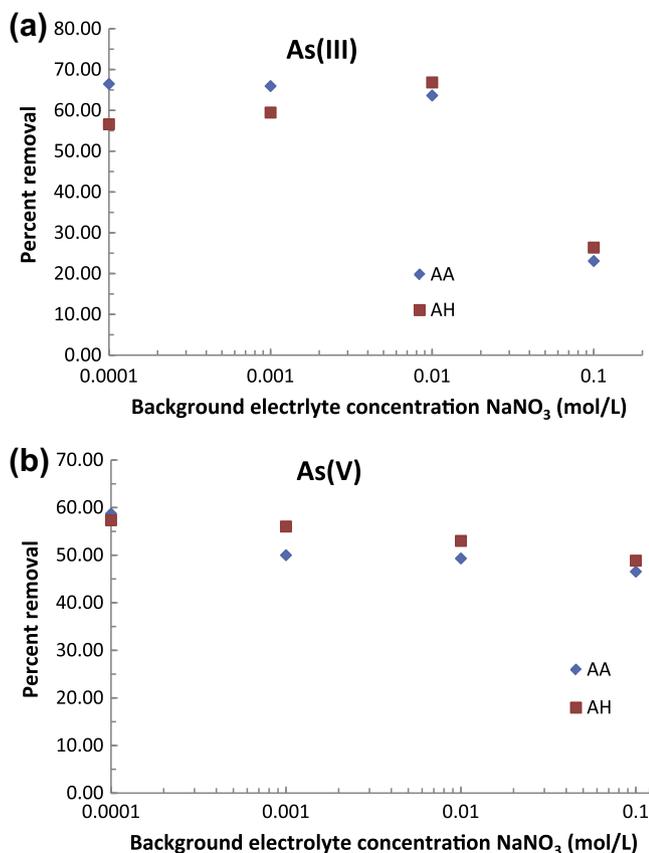
Fig. 6. Effect of background electrolyte concentration in the removal of (a) As(III); and As(V) using inorgano–organo-modified sericite.

Fig. 7. Effect of simultaneous presence of phenol in the removal of (a) As(III); and (b) As(V) using inorgano–organo-modified sericite.

tration indicated that As(III) was mostly sorbed with an electrostatic attraction rather sorbed specifically. Previous, studies also showed that the As(V) was sorbed specifically onto γ-Al$_2$O$_3$ within the pH region 3.0–9.2 whereas As(III) was sorbed un-specifically within the pH region 4.5–9.0 [30,32]. However, As(III) sorption onto the zirconium(IV)oxide-ethanolamine was reported to be ion-exchange along with the electrostatic attraction [31]. Vaishya and Gupta [36] assumed that the major driving force in adsorption of As(III) onto the iron-modified sand was the van der Waals attraction.
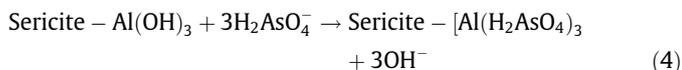
3.4.5. Effect of phenol concentration

Further, the phenol concentration was increased from 0.5 to 2 mg/L and the removal of As(III)/or As(V) was assessed using the materials AH and AA. The studies could enable to view that solids were useful in simultaneous removal of these pollutants. There might be two different domains of active sites capable to sorb inorganic and organic pollutants separately. Results showed that the percent uptake of As(III) was decreased from 42.15% to 40.48%
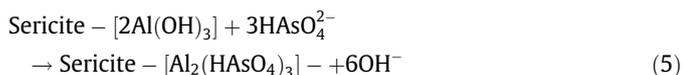
(for AH) and from 40.22% to 30.95% (for AA) samples for the increase of phenol concentration respectively, from 0.5 to 2 mg/L (cf Fig. 7a and b). Whereas the similar increase of phenol concentration caused to decrease of As(V) uptake respectively from 32.75% to 18.22% (for AH) and 35.37% to 25.70% (for AA). These results indicated that insignificant decrease of As(III) or As(V) (maximum of 14.5%) was occurred even with increase of phenol concentration to four times i.e., from 0.5 to 2.0 mg/L. Hence, it was concluded that As(III) or As(V) was sorbed mostly at inorganic sites comparing to the organic end of HDTMA or AMBA. The previous studies described that inorgano–organo-clay i.e., bentonite was modified with Fe polycations and cetyltrimethylammonium bromide (CTMAB) in the simultaneous removal of phosphate and phenanthrene from aqueous solution. They further reported that the solid possessed two different sorption sites capable to remove different types of pollutants i.e., organic and inorganic pollutants from the aqueous solutions simultaneously [17].

The removal mechanism of As(III) or As(V) was suggested as inner sphere complexation with the aluminum ion introduced within the interspace as anion/OH$^-$ exchange reactions [38,43]. Similarly, the adsorption of phosphate was showed specific sorption onto the

free Al or Fe oxides in the soils [44]. The adsorption of As(V) on to ferrihydrite proceeded with surface charge reduction associated with net OH⁻ release. This was suggested to the specific adsorption of As(V), took place onto the surface of metal oxides [45]. X-ray absorption structure spectroscopic studies indicated that the bidentate and binuclear complexes were formed onto γ-Al$_2$O$_3$ with As(V) [30,46,47] whereas inner- and outer-sphere adsorption processes coexist for As(III) onto γ-Al$_2$O$_3$ [30]. Hence keeping these observations and similar previous studies, it was concluded that the As(V) was sorbed specifically with the aluminum oxide introduced within interspace. The ion exchange mechanism could be presented as:

$$\text{Sericite} - \text{Al(OH)}_3 + 3\text{H}_2\text{AsO}_4^- \rightarrow \text{Sericite} - [\text{Al}(\text{H}_2\text{AsO}_4)_3] + 3\text{OH}^- \quad (4)$$

and/or

$$\text{Sericite} - [2\text{Al(OH)}_3] + 3\text{HAsO}_4^{2-} \rightarrow \text{Sericite} - [\text{Al}_2(\text{HAsO}_4)_3] - + 6\text{OH}^- \quad (5)$$

(a) As(III)

Measured-AA
Calculated-AA
Measured-AH
Calculated-AH

C_e/C_0

Throughput volume (L)

(b) As(V)

Measured-AA
calculated-AA
Measured-AH
Calculated-AH

C_e/C_o

Throughput volume (L)

Fig. 8. Breakthrough curves for the removal of (a) As(III); (b) As(V) by inorgano–organo-modified sericite fitted for the Thomas model.

Table 3
Thomas constants for the removal of As(III) and As(V) from aqueous solutions by inorgano–organo-modified sericite.

| Systems	q_0 (mg/g)	$K_T \times 10^{-3}$ (L/min/mg)
As(III)-AA	0.338	6.76
As(III)-AH	0.433	6.48
As(V)-AA	0.541	5.99
As(V)-AH	0.852	4.12

On the other hand the As(III) was sorbed at the solid surface by an electrostatic or even van der Waals type of attraction.

3.5. Breakthrough curves for As(III) and As(V)

The applicability of the AA and AH hybrid materials was further assessed in the removal of As(III) and As(V) under the dynamic conditions. These data were found to be direct practical implication of these materials in the possible large scale or pilot scale treatment of water contaminated with arsenic. The column conditions were maintained as stated before and the results obtained were presented graphically in Fig. 8a and b respectively for the As(III) and As(V). It was interesting to note that complete breakthrough was occurred for As(III) at the throughput volume of 0.357 L for AA and 0.393 L for AH solids. Similarly, it was observed for the As(V) at 0.483 L for AA and 0.756 L for AH solids. These results indicated that AH showed better suitability for the removal of As(III) or As(V) from aqueous solutions. Further, the breakthrough data was used for the non-linear fitting to the Thomas equation (Eq. (3)) in order to optimize the two unknown parameters viz., q_0 and K_T. Reasonably a good fitting of breakthrough curve was obtained for these systems as shown in Fig. 8a and b with the calculated lines. Similar results were also reported previously using the biosorbents or manganese coated sands, etc. [24,48,49]. The Thomas constants i.e., q_0 and K_T were estimated for these solids and were presented in Table 3. Table clearly demonstrated that the solid AH possessed with better removal capacity for As(III) or As(V) compared to the AA solid. These results were in accordance to the batch reactor data obtained previously.

4. Conclusions

The novel inorgano–organo-sericite materials were obtained in the laboratory and assessed for its applicability in the removal of As(III) and As(V) from aqueous solutions. The aluminum and HDTMA/or AMBA modified sericite was characterized with the help of IR and XRD analytical data. The morphological images showed that very compact layered sericite was become more disordered and heterogeneous in presence of these inorgano–organo ions. The batch reactor data enabled that the removal of these two ions were greatly affected with pH. Presence of background electrolyte concentrations i.e., NaNO$_3$ greatly affected the removal of As(III) whereas it was almost unaffected for As(V). Increase in sorptive concentration apparently enhanced with amount removed however, the percent removal was decreased. The equilibrium modeling showed the applicability of linear and non-linear Freundlich and Langmuir adsorption isotherm. The presence of phenol concentration pointed it that the solid possessed with two different types of active sites endured to two different types of pollutants. The mechanism of As(V) was suggested with the specific sorption (inner sphere complexation) occurred with OH⁻ release, whereas As(III) was sorbed mostly by the electrostatic or even van der Waals type of attraction. The column reactor data fitted well with the Thomas equation and therefore, the maximum amount of As(III) or As(V) to be loaded in the column under the
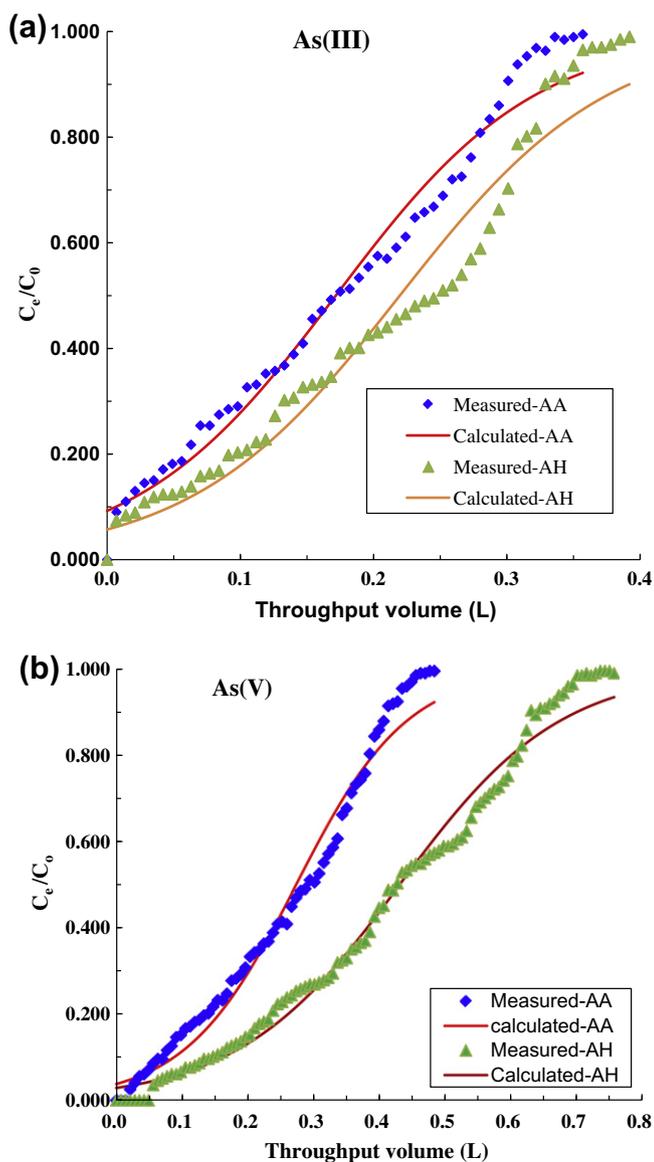
specified column conditions was optimized which indicated that a significant amount of As(III) or As(V) could be loaded in the column. These results further pointed the potential use of these materials, in particular the treatment of arsenic contaminated waters. Further, comparing these two solids studied, AH possessed with higher removal capacity than the AA at least in the removal of As(III) or As(V).

References

[1] M.M. Karim, Arsenic in groundwater and health problems in Bangladesh, Wat. Res. 34 (2000) 304–310.
[2] D. Mohan, C.U. Pittman Jr., Arsenic removal from water/wastewater using adsorbents – a critical review, J. Haz. Mater. 142 (2007) 1–53.
[3] P. Mondal, C.B. Majumder, B. Mohanty, Laboratory based approaches for arsenic remediation from contaminated water: recent developments, J. Haz. Mater. 13 (2006) 464–479.
[4] E.T. Mackenzie, R.J. Lamtzy, V. Petorson, Global trace metals cycles and predictions, J. Int. Assoc. Math. Geol. 6 (1979) 99–142.
[5] C.K. Jain, I. Ali, Arsenic: occurrence, toxicity and speciation techniques, Wat. Res. 34 (2000) 4304–4312.
[6] J.M. Desesso, C.F. Jacobson, A.R. Scialli, C.H. Farr, J.F. Holson, An assessment of the developmental toxicity of inorganic arsenic, Reprod. Toxic. 12 (1998) 385–433.
[7] A.A. Duker, E.J.M. Carranza, M. Hal, Arsenic geochemistry and health, Environ. Int. 31 (2005) 631–641.
[8] J.C. Ng, J. Wang, A. Shraim, A global health problem caused by arsenic from natural sources, Chemosphere 52 (2003) 1353–1359.
[9] M.D. Kiping, Arsenic, the chemical environment, environment and man, in: J. Lenihan, W.W. Fletcher, (Eds.), Glasgow, vol. 6, 1997, pp. 93–110.
[10] B.K. Mandal, K.T. Suzuki, Arsenic round the world: a review, Talanta 58 (2002) 201–235.
[11] S.M. Lee, D. Tiwari, Organo and inorgano–organo-modified clays in the remediation of aqueous solutions: an overview, Appl. Clay Sci. 59–60 (2012) 84–102.
[12] Z. Li, R.S. Bowman, Retention of inorganic oxyanions by organo-kaolinite, Wat. Res. 35 (2001) 3771–3776.
[13] L. Zhu, S. Tian, J. Zhu, Y. Shi, Silylated pillared clay (SPILC): a novel bentonite-based inorgano–organo composite sorbent synthesized by integration of pillaring and silylation, J. Colloid Interf. Sci. 315 (2007) 191–199.
[14] Y. El-Nahhal, S. Nir, T. Polubesova, L. Margulis, B. Rubin, Leaching, phytotoxicity and weed control of new formulations of alachlor, J. Agric. Food Chem. 46 (1998) 3305–3313.
[15] O. Bouras, T. Chami, M. Houari, H. Khalaf, J.C. Bollinger, M. Baudu, Removal of sulfacid brilliant pink from an aqueous stream by adsorption onto surfactant-modified Ti-pillared montmorillonite, Environ. Technol. 23 (2002) 405–411.
[16] O. Bouras, M. Houari, H. Khalaf, Using of surfactant modified Fe-pillared bentonite for the removal of pentachlorophenol from aqueous stream, Environ. Technol. 22 (2001) 69–74.
[17] J. Ma, L. Zhu, Simultaneous sorption of phosphate and phenanthrene to inorgano–organo-bentonite from water, J. Haz. Mater. B136 (2006) 982–988.
[18] L. Yan, X. Shan, B. Wen, S. Zhang, Effect of lead on the sorption of phenol onto montmorillonites and organo-montmorillonites, J. Colloids Interf. Sci. 308 (2007) 11–19.
[19] Z. Bouberka, H.A.M. Khenifi, B. Haddou, N. Belkaid, N. Bettahar, Z. Derriche, Adsorption of supranol yellow 4GL from aqueous solution by surfactant-treated aluminum/chromium-intercalated bentonite, J. Haz. Mater. 162 (2009) 378–385.
[20] O. Bouras, J.C. Bollinger, M. Baudu, H. Khalaf, Adsorption of diuron and its degradation products from aqueous solution by surfactant modified pillared clays, Appl. Clay Sci. 37 (2007) 240–250.
[21] D. Tiwari, H.U. Kim, S.M. Lee, Removal behavior of sericite for Cu(II) and Pb(II) from aqueous solutions: batch and column studies, Sep. Purif. Technol. 57 (2007) 11–16.
[22] D. Tiwari, M. Kim, W.G. Kim, S. M. Lee, Organo-sericite in the remediation of phenol contaminated waters. in: Proceedings of 3rd IWA Asia Pacific Young Water Professionals International Conference, Singapore, 2010.
[23] S.M. Lee, D. Tiwari, K.M. Choi, J.K. Yang, Y.Y. Chang, H.D. Lee, Removal of Mn(II) from aqueous solutions using manganese-coated sand samples, J. Chem. Eng. Data 54 (2009) 1823–1828.
[24] D. Tiwari, C. Laldanwngliana, C.H. Choi, S.M. Lee, Manganese-modified natural sand in the remediation of aquatic environment contaminated with heavy metal toxic ions, Chem. Eng. J. 171 (2011) 958–966.
[25] S.J. Allen, G. Mckay, J.F. Porter, Adsorption isotherm models for basic dye adsorption by peat in single and binary component systems, J. Colloids Interface Sci. 280 (2004) 322–333.
[26] H.C. Thomas, Heterogeneous ion exchange in a flowing system, J. Am. Chem. Soc. 66 (1944) 1664–1666.
[27] U.F. Alkaram, A.A. Mukhlis, A.H. Al-Dujaili, The removal of phenol from aqueous solutions by adsorption using surfactant-modified bentonite and kaolinite, J. Haz. Mater. 169 (2009) 324–332.
[28] J.M. Trilo, M.D. Alba, A.A. Castro, A. Munoj, J. Poyato, M. Tobias, Local environment of lanthanum ions in montmorillonite upon heating, Clay Miner. 27 (1992) 423–434.
[29] S.E. Miller, G.R. Heath, R.D. Gonzalez, Effects of temperature on the sorption of lanthanides by montmorillonite, Clays Clay Miner. 30 (1982) 111–122.
[30] B.G. Mishra, G.R. Rao, Physicochemical and catalytic properties of Zr-pillared montmorillonite with varying pillar density, Mesopor. Micropor. Mater. 70 (2004) 43–50.
[31] C.V. Farmer, Spectra of Minerals, Mineralogical Society, London, 1974.
[32] S.M. Koh, J.B. Dixon, Preparation and application of organo-minerals as sorbents of phenol, benzene and toluene, Appl. Clay Sci. 18 (2001) 111–122.
[33] Y. Arai, E.J. Elzinga, D.L. Sparks, X-ray adsorption spectroscopic investigation of arsenite and arsenate adsorption at the aluminum oxide–water interface, J. Colloid Interface Sci. 235 (2001) 80–88.
[34] S. Mandal, T. Padhi, R.K. Patel, Studies on the removal of arsenic(III) from water by a novel hybrid material, J. Haz. Mater. 192 (2011) 899–908.
[35] R.K. Xu, Y. Wang, D. Tiwari, H. Wang, Effect of ionic strength on adsorption of As(III) and As(V) on variable charge soils, J. Environ. Sci. 21 (2009) 927–932.
[36] R.C. Vaishya, S.K. Gupta, Modelling arsenic(III) adsorption from water by sulfate modified iron-oxide coated sand (SMIOCS), Sep. Sci. Technol. 39 (2004) 645–666.
[37] Y.Y. Chang, S.M. Lee, J.K. Yang, Removal of As(III) and As(V) by natural and synthetic metal oxides, Colloids Surf. A: Physicochem. Eng. Asp. 346 (2009) 202–207.
[38] Y.H. Xu, T. Nakajima, A. Ohki, Adsorption and removal of arsenic(V) from drinking water by aluminum-loaded Shirasu-zeolite, J. Haz. Mater. B92 (2002) 275–287.
[39] P. Benes, V. Majer, Trace Chemistry of Aqueous Solutions, Elsevier, Amsterdam, 1980.
[40] S.P. Mishra, D. Tiwari, R.S. Dubey, Biosorptive behavior of casein for Zn^{2+}, Hg^{2+} and Cr^{3+}: effects of physic-chemical treatments, Bioresour. Technol. 63 (1998) 1–5.
[41] V.K. Gupta, V.K. Saini, N. Jain, Adsorption of As(III) from aqueous solutions by iron oxide-coated sand, J. Colloid Interf. Sci. 288 (2005) 55–60.
[42] K.F. Hayes, C. Papelis, J.O. Leckie, Modeling ionic strength effects on anion adsorption at hydrous oxide/solution interfaces, J. Colloid Interf. Sci. 125 (1988) 717–726.
[43] J. Antelo, M. Avena, S. Fiol, R. L'opez, F. Arce, Effects of pH and ionic strength on the adsorption of phosphate and arsenate at the goethite–water interface, J. Colloid Interf. Sci. 285 (2005) 476–486.
[44] Y. Wang, Jiang. Xu, J. Ren-kou, D. Tiwari, Phosphate adsorption at variable charge soil/water interfaces as influenced by ionic strength, Aust. J. Soil Res. 47 (2009) 529–536.
[45] A. Jain, K.P. Raven, R.H. Loeppert, Arsenite and arsenate adsorption on ferrihydrite: surface charge reduction and net OH^- release stoichiometry, Environ. Sci. Technol. 33 (1999) 1179–1184.
[46] S.E. Fendorf, M.J. Eick, P. Grossl, D.L. Sparks, Arsenate and chromate retention mechanism on goethite. 1. Surface structure, Environ. Sci. Technol. 31 (1997) 315–320.
[47] G.A. Waychunas, B.A. Rea, C.C. Fuller, J.A. Davis, Surface chemistry of ferrihydrite: Part 1. EXAFS studies of the geometry of coprecipitated and adsorbed arsenate, Geochim. Cosmochim. Acta 57 (1993) 2251–2269.
[48] A. Singh, D. Kumar, J.P. Gaur, Continuous metal removal from solution and industrial effluents using *Spirogyra* biomass-packed column reactor, Wat. Res. 46 (2012) 779–788.
[49] G. Yan, T. Viraraghavan, Heavy metal removal in a biosorption column by immobilized *M. rouxii* biomass, Bioresour. Technol. 78 (2011) 243–249.